Supplement of Atmos. Chem. Phys., 24, 3445–3528, 2024
https://doi.org/10.5194/acp-24-3445-2024-supplement

Atmospheric Chemistry and Physics
Open Access
EGU

Supplement of

Desorption lifetimes and activation energies influencing gas–surface interactions and multiphase chemical kinetics

Daniel A. Knopf et al.

Correspondence to: Daniel A. Knopf (daniel.knopf@stonybrook.edu) and Manabu Shiraiwa (m.shiraiwa@uci.edu)

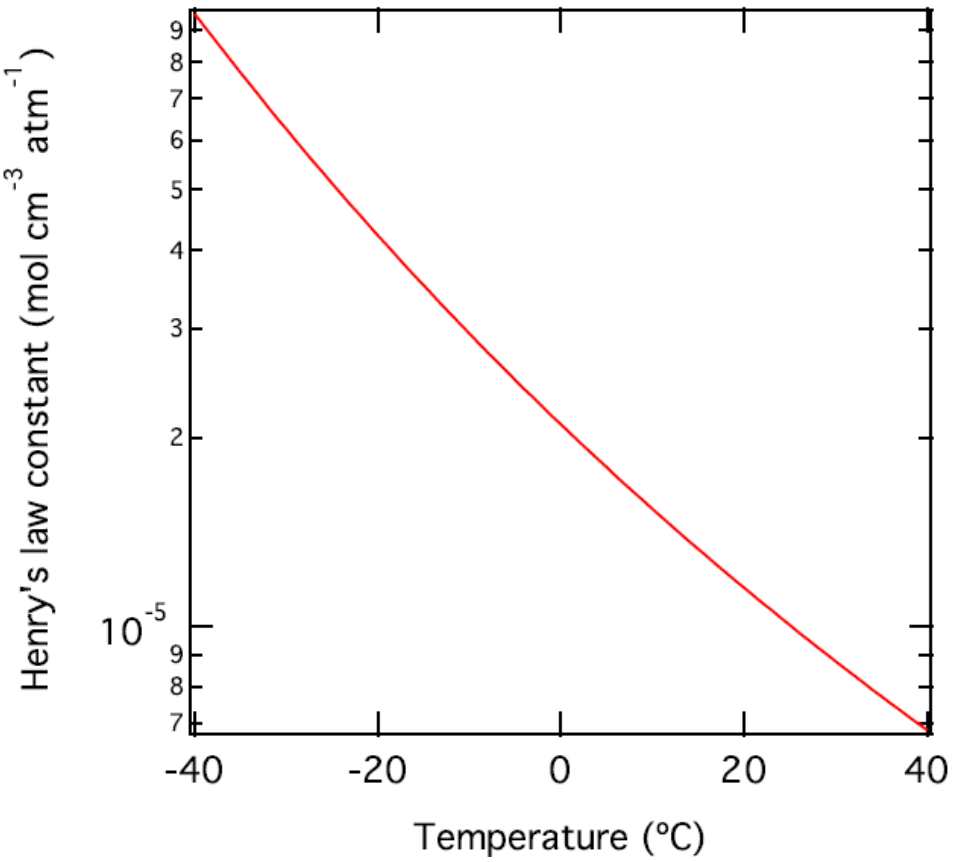

Figure S1. The temperature dependence of the Henry's law coefficient is shown using the van't Hoff equation with solvation enthalpy of 20 kJ mol^{-1}.

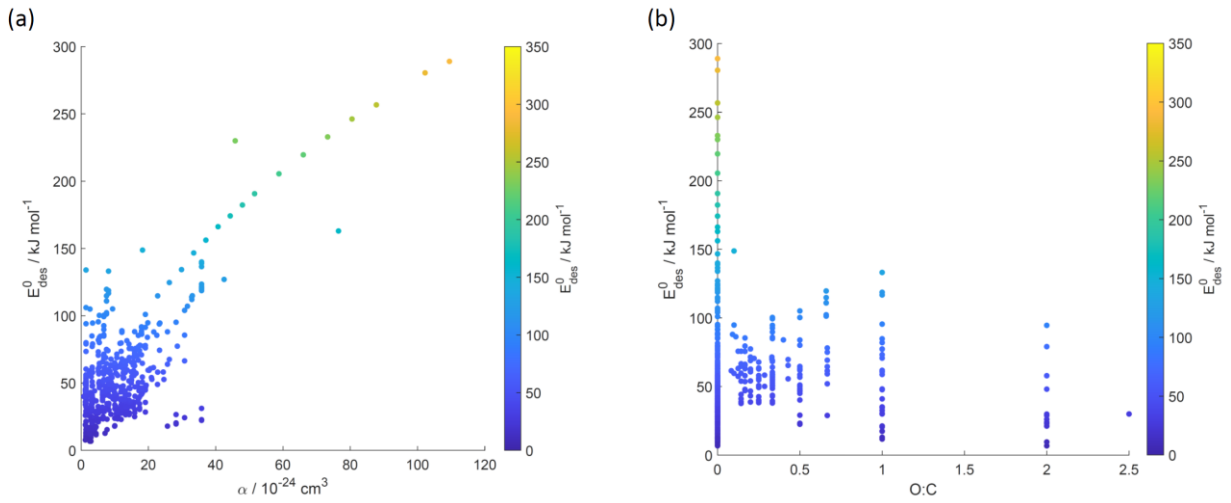

Figure S2. Desorption energy (E^0_{des}) as a function of gas species polarizability (α) in panel (a) and as a function of oxidation state of gas species expressed as $O{:}C$ (b) using data from Tables A1-A15. Panels (a) and (b) reflect data from Fig. 8.

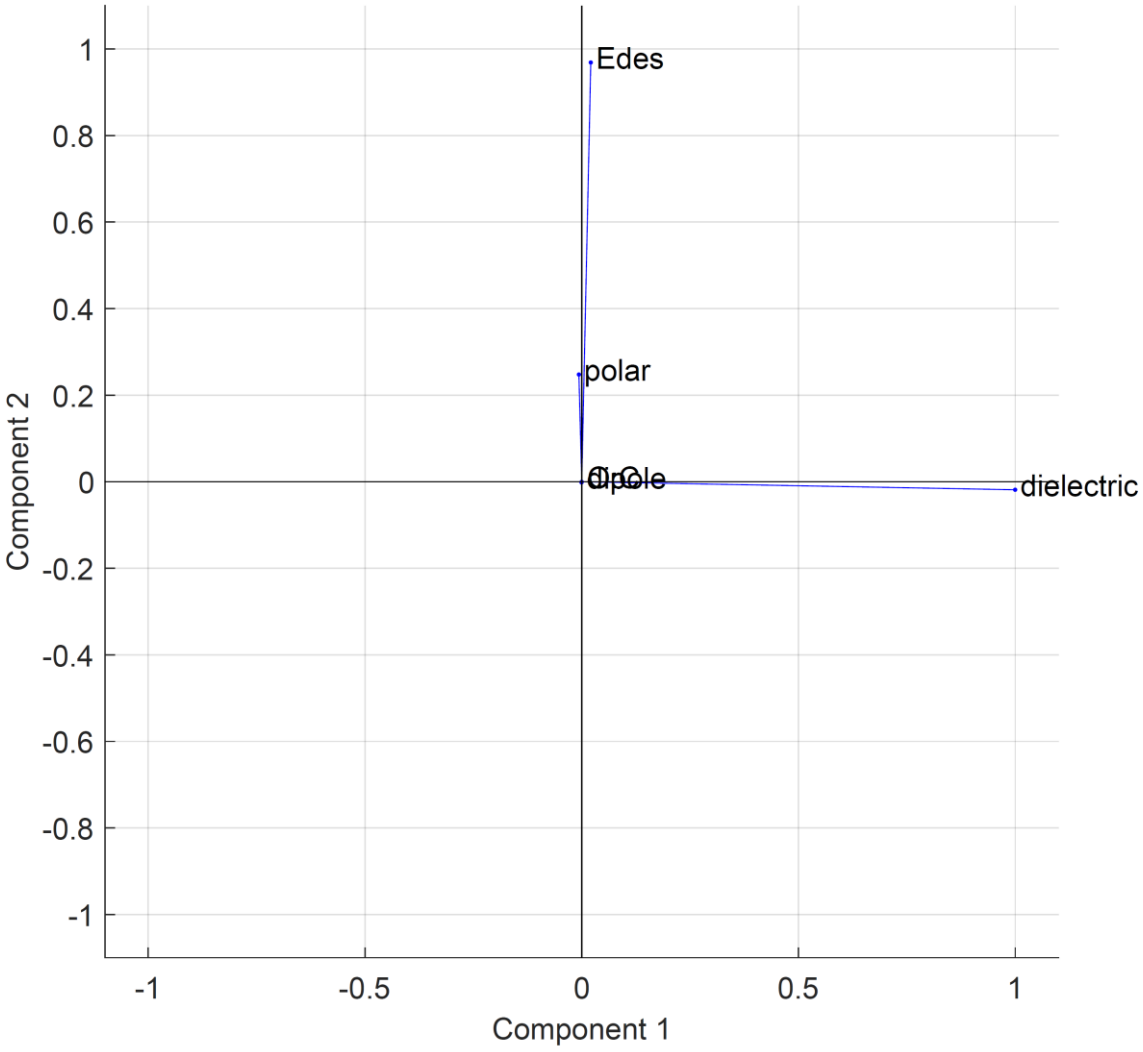

Figure S3. Coefficients derived from principal component analysis to examine the dependencies between the desorption energy (E_{des}^{0}), polarizability (polar, α), dipole moment (dipole, μ), oxygen to carbon ratio ($O{:}\,C$), and relative permittivity of the substrates (dielectric, ε_r).

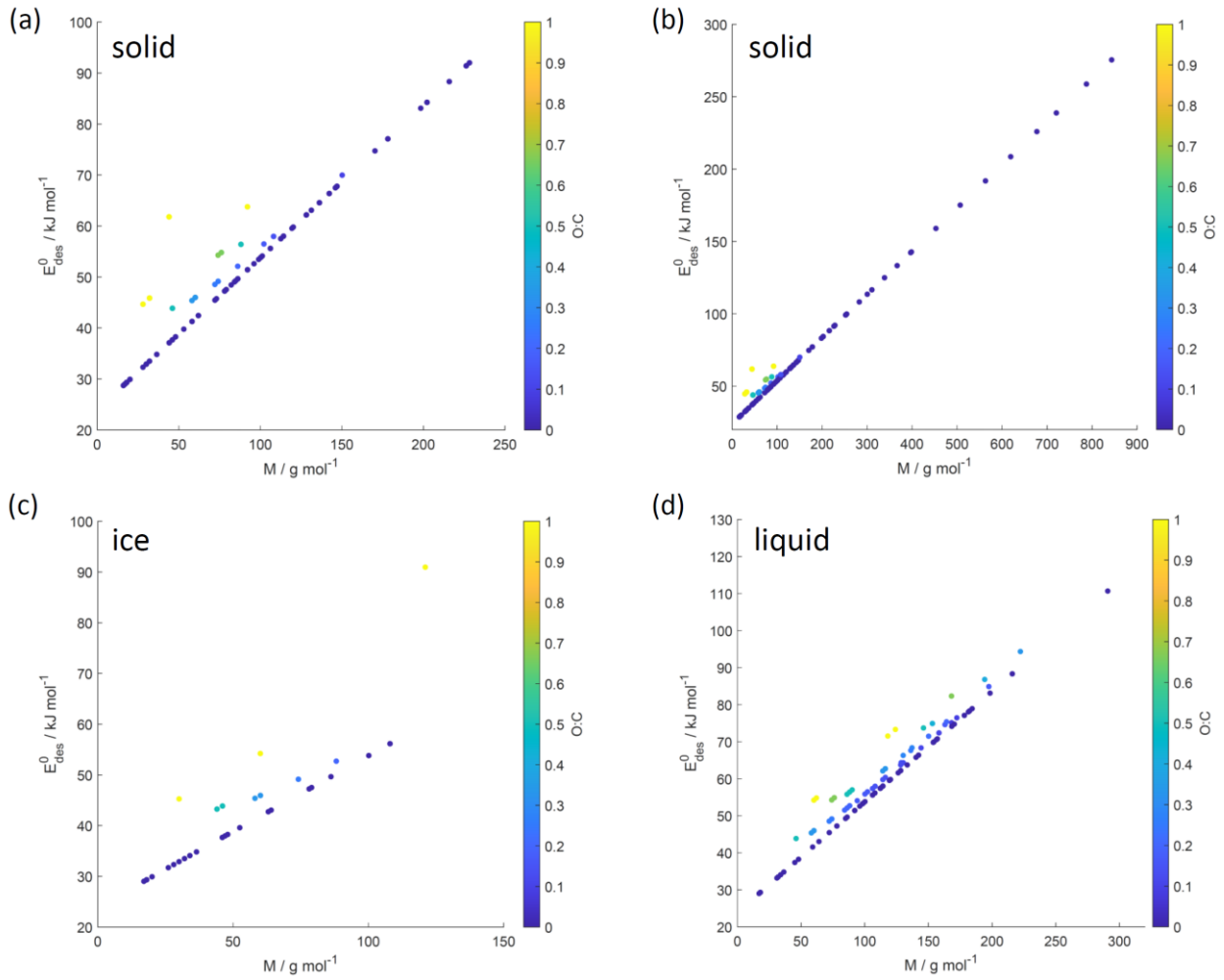

Figure S4. E^0_{des} values derived from the new parameterization (Eq. (17)) applying the training dataset of gas species with molar mass (M) and $O{:}C$, the latter coded as symbol color described by the color bar, similar to Fig. 8. Panels (a) and (b) show data for solid substrates where (a) is an enlarged view of (b). Panel (c) shows data for ice substrates and panel (d) represents the case of liquid substrates. Note that three gas species with $O{:}C > 1$ (CO_2, formic acid, and peroxyacetyl nitrate) are included in these plots as having $O{:}C = 1$ to allow for better visualization of entire data set.

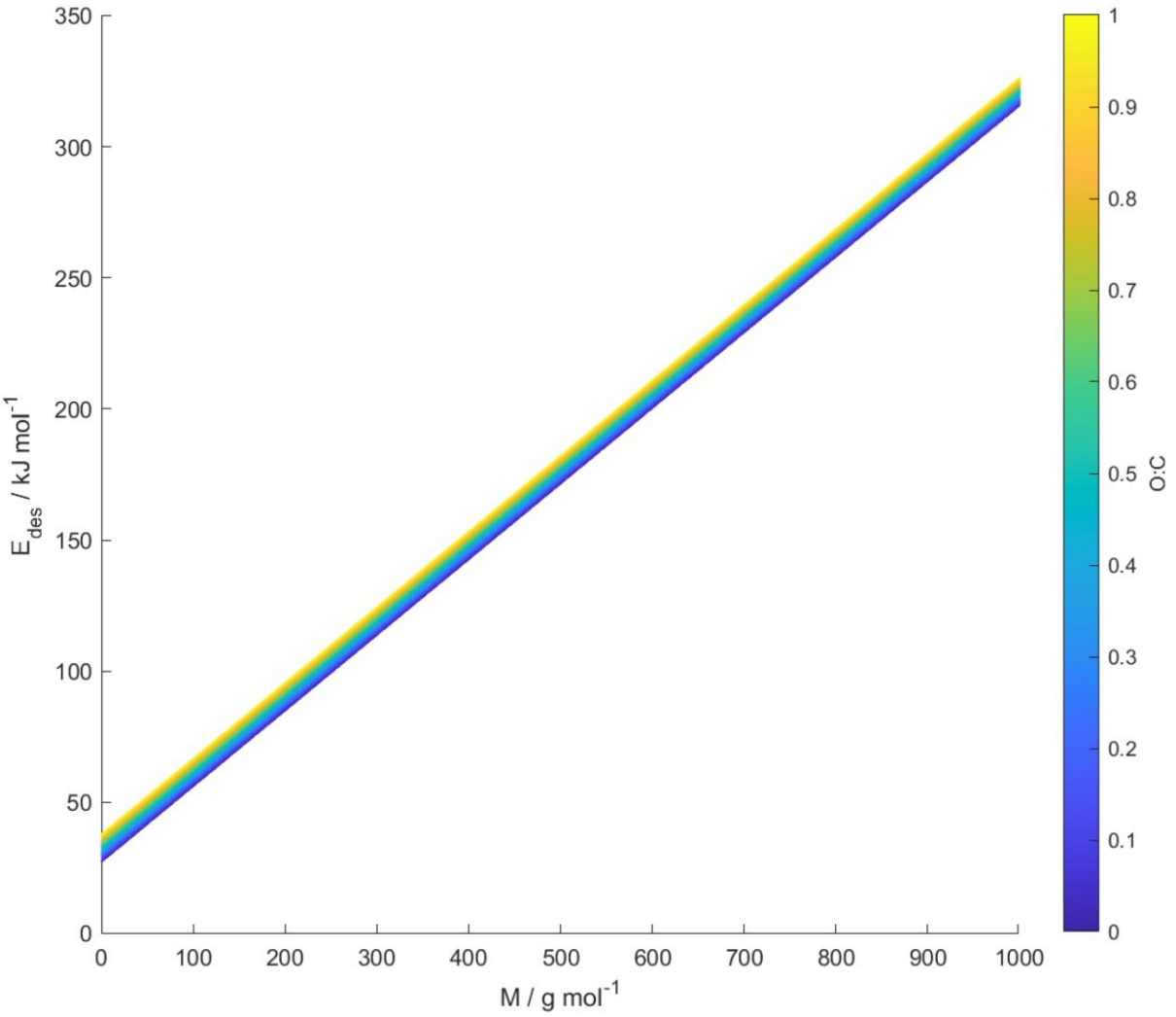

Figure S5. E^0_{des} values derived from the new parameterization (Eq. (17)) applying arbitrary values of molar mass (M) and $O{:}C$, the latter coded as symbol color described by the color bar.

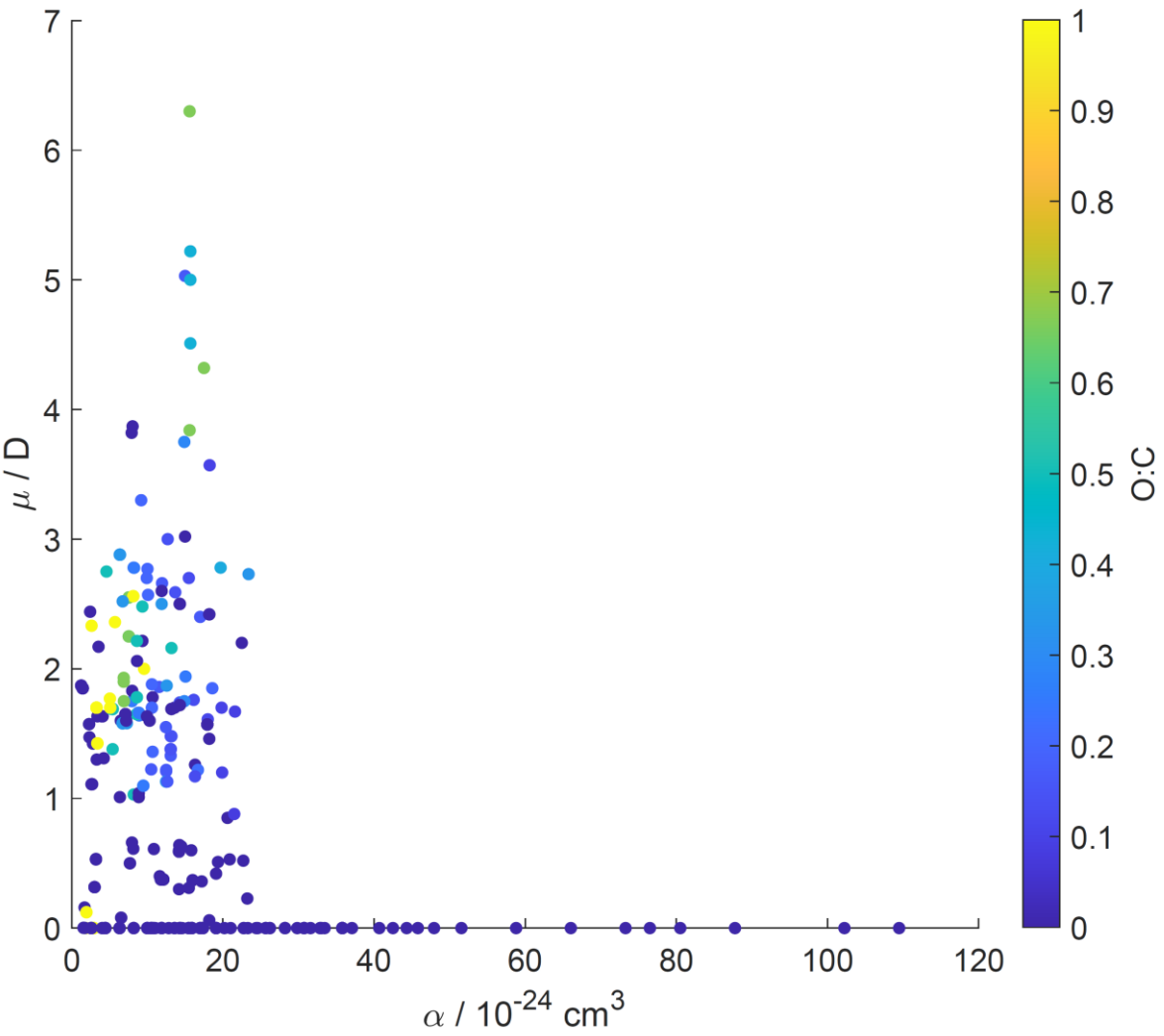

Figure S6. The dipole moment (μ) is plotted against the polarizability (α) where color shading indicates the oxidation state ($O:C$). Note that three gas species with $O:C > 1$ (CO_2 and formic acid) are included in this plot as having $O:C = 1$ to allow for better visualization of entire data set.

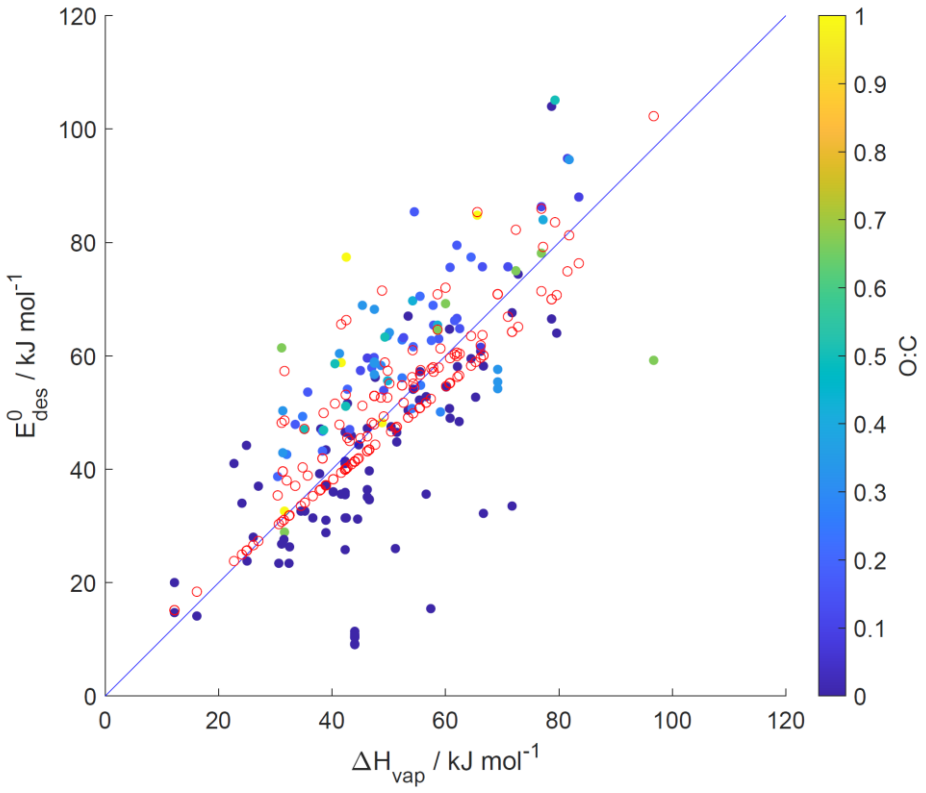

Figure S7. Same as Fig. 11c. Red open circles depict the linear regression model applying the training data set: $E^0_{\mathrm{des}}(\Delta H_{\mathrm{vap}}, O{:}C) = 5.0711 + 0.8247\Delta H_{\mathrm{vap}} + 26.1822(O{:}C)$ with an R^2 = 0.56 and RMSE = 13.0.

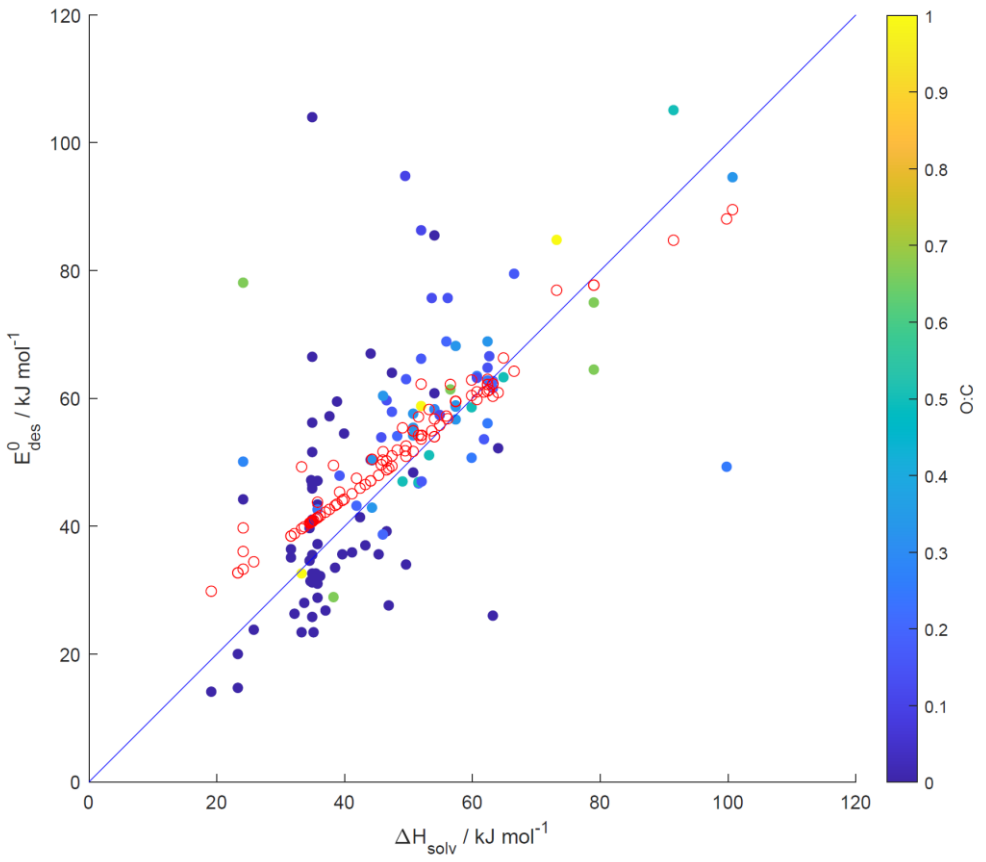

Figure S8. Same as Fig. 12. Red open circles depict the linear regression model applying the training data set: $E^0_{\mathrm{des}}(\Delta H_{\mathrm{solv}}, O{:}C) = 16.5830 + 0.6923\Delta H_{\mathrm{solv}} + 9.6772(O{:}C)$ with an R^2 = 0.39 and RMSE = 14.3.

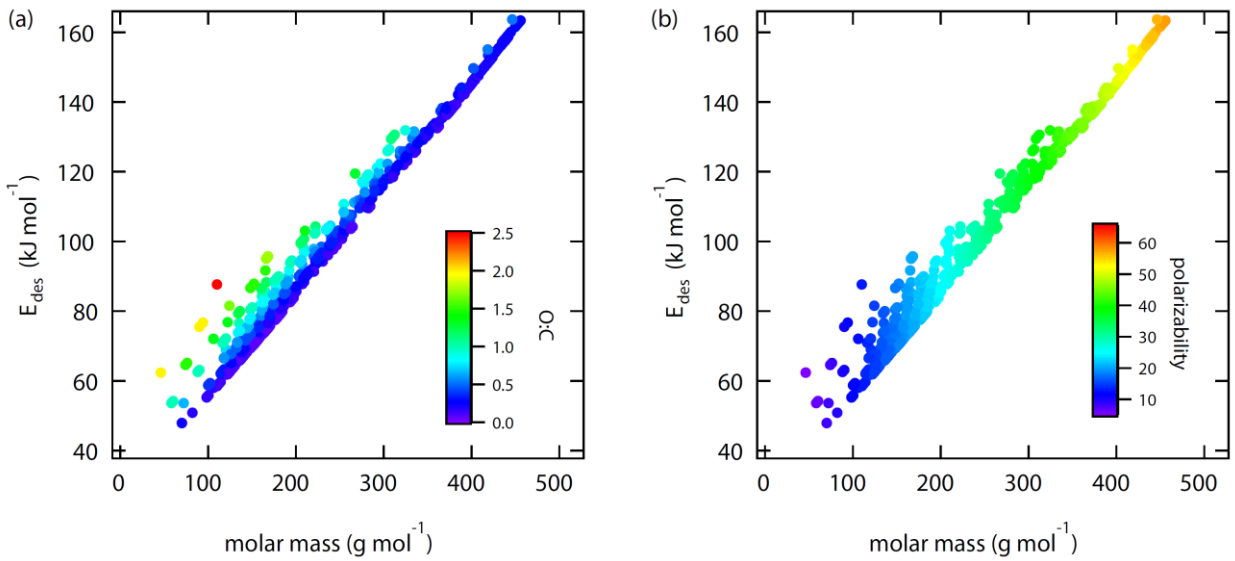

Figure S9. Calculated desorption energies (E^0_{des}) of SOA precursor gases from (Shiraiwa et al., 2014) as a function molar mass and its dependence on $O{:}C$ (a) and polarizability (b) using parameterization Eq. (17).

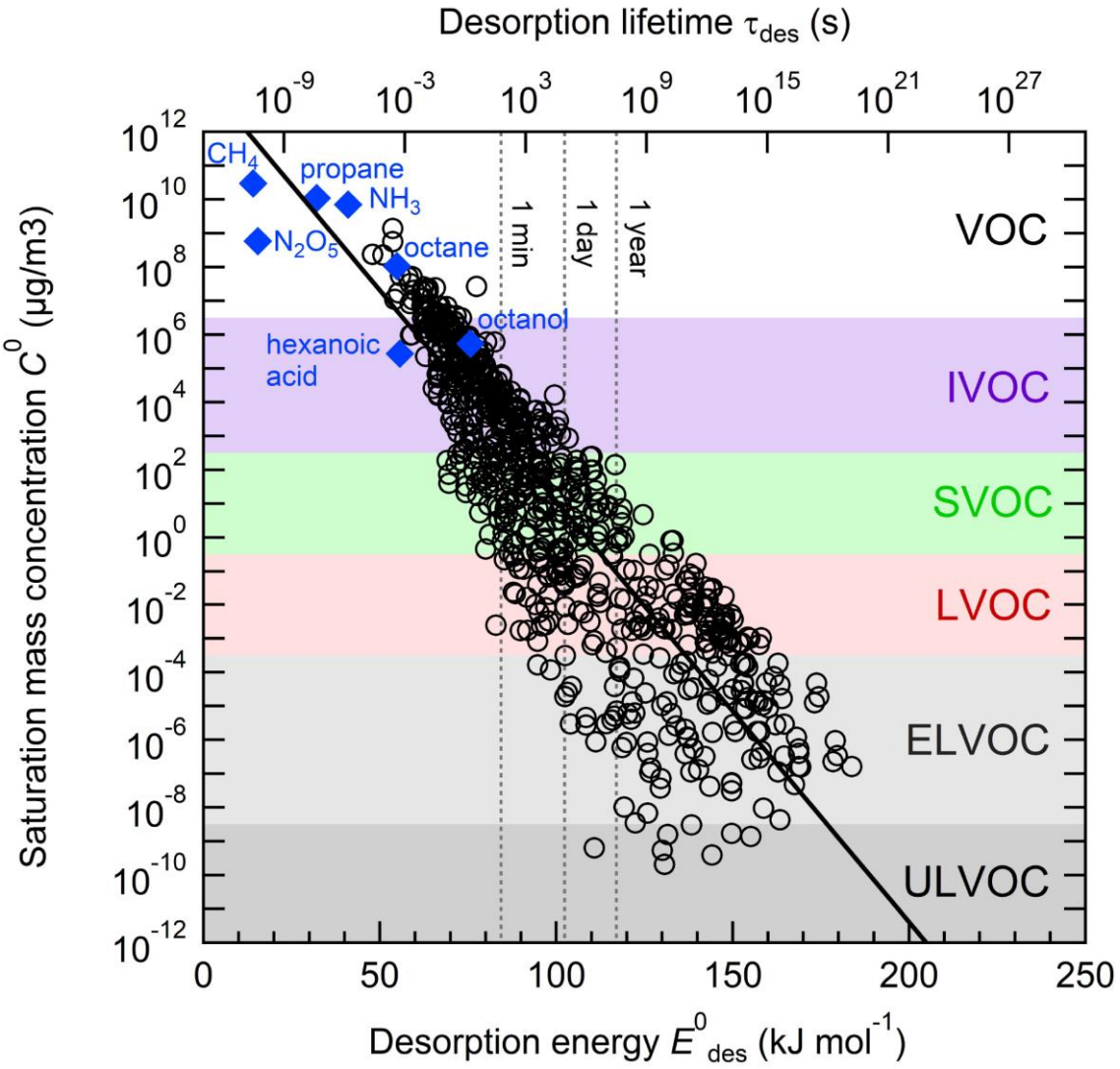

Figure S10. Characteristic desorption energies (E^0_{des}), desorption lifetimes (τ_{des}), and saturation mass concentration (C^0) at 298 K for secondary organic aerosol (SOA) components and other selected compounds of atmospheric relevance. The blue markers show experimental literature data of E^0_{des} and C^0. The black markers correspond to the molecular corridor data of SOA formation displayed in Fig. 13 (Shiraiwa et al., 2014), for which C^0 was estimated with the EVAPORATION model (Compernolle et al., 2011) and a constant conversion factor of 10^{-10} atm m^3 µg^{-1} (see text) and E^0_{des} was estimated using Eq. (15). The black solid line represents an exponential fit to the SOA molecular corridor data. Blue markers show experimental data for selected other compounds of atmospheric relevance. Color shadings indicate widely used categories of SOA volatility basis set (VBS): volatile organic compounds (VOC), semi-volatile organic compounds (SVOC), low volatility organic compounds (LVOC), extremely-low volatility organic compounds (ELVOC) and ultra-low volatility organic compounds (ULVOC) (Schervish and Donahue, 2020; Donahue et al., 2009).

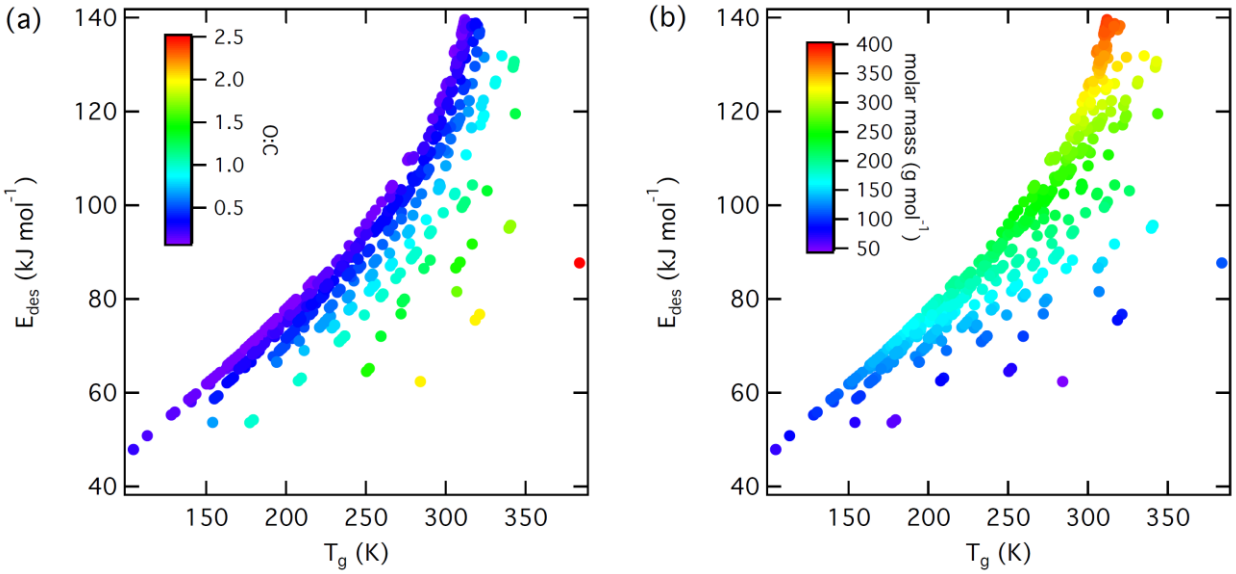

Figure S11. Relationship between calculated desorption energies (E^0_{des}) of SOA precursor gases from Shiraiwa *et al.* (2014) and species' glass transition temperature (T_g) and its dependence on $O{:}C$ (a) and molar mass (b) using parameterization Eq. (17).

References

Compernolle, S., Ceulemans, K., and Muller, J. F.: EVAPORATION: a new vapour pressure estimation methodfor organic molecules including non-additivity and intramolecular interactions, Atmos. Chem. Phys., 11, 9431-9450, 10.5194/acp-11-9431-2011, 2011.

Donahue, N. M., Robinson, A. L., and Pandis, S. N.: Atmospheric organic particulate matter: From smoke to secondary organic aerosol, Atmos. Environ., 43, 94-106, 10.1016/j.atmosenv.2008.09.055, 2009.

Schervish, M. and Donahue, N. M.: Peroxy radical chemistry and the volatility basis set, Atmos. Chem. Phys., 20, 1183-1199, 10.5194/acp-20-1183-2020, 2020.

Shiraiwa, M., Berkemeier, T., Schilling-Fahnestock, K. A., Seinfeld, J. H., and Pöschl, U.: Molecular corridors and kinetic regimes in the multiphase chemical evolution of secondary organic aerosol, Atmos. Chem. Phys., 14, 8323-8341, 10.5194/acp-14-8323-2014, 2014.